ACS Chemical Neuroscience

Letter

pubs.acs.org/chemneuro

Development of a Photoactivatable Allosteric Ligand for the M_1 Muscarinic Acetylcholine Receptor

Briana J. Davie,[†,‡] Patrick M. Sexton,[‡] Ben Capuano,[†] Arthur Christopoulos,*[,‡] and Peter J. Scammells*[,†]

[†]Medicinal Chemistry and [‡]Drug Discovery Biology, Monash Institute of Pharmaceutical Sciences, Monash University, Parkville, Victoria 3052, Australia

Supporting Information

ABSTRACT: The field of G protein-coupled receptor drug discovery has benefited greatly from the structural and functional insights afforded by photoactivatable ligands. One G protein-coupled receptor subfamily for which photoactivatable ligands have been developed is the muscarinic acetylcholine receptor family, though, to date, all such ligands have been designed to target the orthosteric (endogenous ligand) binding site of these receptors. Herein we report the synthesis and pharmacological investigation of a novel photoaffinity label, MIPS1455 (**4**), designed to bind irreversibly to an allosteric site of the M_1 muscarinic acetylcholine receptor; a target of therapeutic interest for the treatment of cognitive deficits. MIPS1455 may be a valuable molecular tool for further investigating allosteric interactions at this receptor.

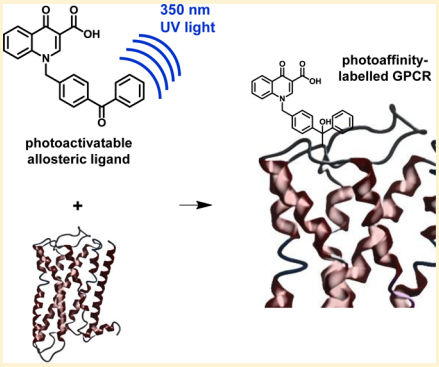

KEYWORDS: *Muscarinic, allosteric, photoactivatable, photoaffinity, BQCA, cognition*

Photoaffinity labeling is a robust technique that is highly amenable to the study of ligand interactions with G protein-coupled receptors (GPCRs).[1] The utility of photoaffinity labeling arises from the range of photoactivatable functionalities available for incorporation into both ligands and receptors,[2] the potential for applying this technique to study any ligand−receptor[1] or, indeed, receptor−receptor complex,[3] and the ability to use the technique in tandem with more recently developed computational, genetic, and crystallographic technologies.

Photoaffinity labeling involves taking a known ligand or receptor and incorporating a photoactivatable moiety; a functional group capable of forming a reactive species (typically a carbene, nitrene, or diradical) upon electronic excitation at a specific wavelength of ultraviolet (UV) light. This species is then able to rapidly react or "cross-link" with a chemical bond of a neighboring entity in close proximity. Photoactivatable ligands offer the significant advantage of temporal control of reactivity, compared to affinity-labeled ligands containing, for example, inherently reactive electrophilic functionalities. The receptor may be pretreated with the "ground state" ligand prior to photoactivation, increasing the likelihood of "capturing" the ligand−receptor complex of interest. However, as with affinity-labeled ligands, reasonable affinity for the receptor and a similar pharmacological profile to the parent molecule are important to ensure selective labeling of the binding site of interest.[4]

Photoactivatable functionalities that are routinely incorporated into known ligands include benzophenones, diazirines and aryl azides (Figure 1).[5] Benzophenone-containing probes undergo photoactivation at 350−360 nm and have the notable advantages of higher chemical stability and higher cross-linking efficiency compared to diazirines and aryl azides. However, their bulk means that they may result in a less accurate representation of the parent ligand−receptor interaction. Diazirines and aryl azides are hence more prudent choices if incorporation of a benzophenone is likely to result in steric clashes with the binding pocket.

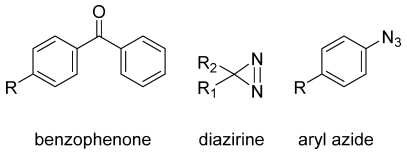

Figure 1. Three commonly used photoactivatable functionalities.

Diazirines, which photoactivate at 350−380 nm, may also prove to be an advantageous choice if considerable nonspecific cross-linking is anticipated; they display low cross-linking efficiency such that a covalent complex will only form if the ligand has very high affinity for the receptor.[5] A considerable drawback is that their synthesis can be complicated and time-consuming. Aryl azides, while more synthetically accessible that diazirines, require photoirradiation at <300 nm; wavelengths likely to cause nonspecific damage to the biological system under investigation.[6]

Photoaffinity labeling has considerably advanced our understanding of ligand−receptor and receptor−receptor interactions at Family A GPCRs. The technique has enabled the identification and structural characterization of ligand binding sites,[1,7] provided early evidence for receptor dimerization,[3] and

Published: September 4, 2014

   dx.doi.org/10.1021/cn500173x | ACS Chem. Neurosci. 2014, 5, 902−907

facilitated receptor purification that has subsequently aided GPCR crystallization.[8] Muscarinic acetylcholine receptors (mAChRs) are Family A GPCRs that, due to their widespread expression in the central nervous system,[9] have been extensively investigated as therapeutic targets for enhancing cognition and alleviating psychotic symptoms in conditions such as schizophrenia and Alzheimer's disease.[10] Examples of photoactivatable ligands for mAChRs include aryl azide derivatives of the potent orthosteric antagonists tropine,[11] 3-quinuclidinyl benzilate (3QNB),[12] and *N*-methyl-4-piperidyl benzilate (4NMPB).[12,13] In addition to the highly structurally conserved orthosteric ligand binding site, the existence of multiple, topographically distinct allosteric ligand binding sites at mAChRs has been extensively experimentally validated.[14] While an array of mAChR allosteric ligands have subsequently been developed,[15] our knowledge about the precise location and structure of their binding sites and the interactions of allosteric ligands within them is in its infancy. Hence, photoactivatable ligands for allosteric sites may be of significant worth to this field of research.

Herein we describe the development of a photoactivatable irreversible allosteric ligand, MIPS1455 (**4**, Figure 2), for the M_1 mAChR that may be useful in further probing the structural and functional mechanisms governing allosteric ligand-mAChR interactions.

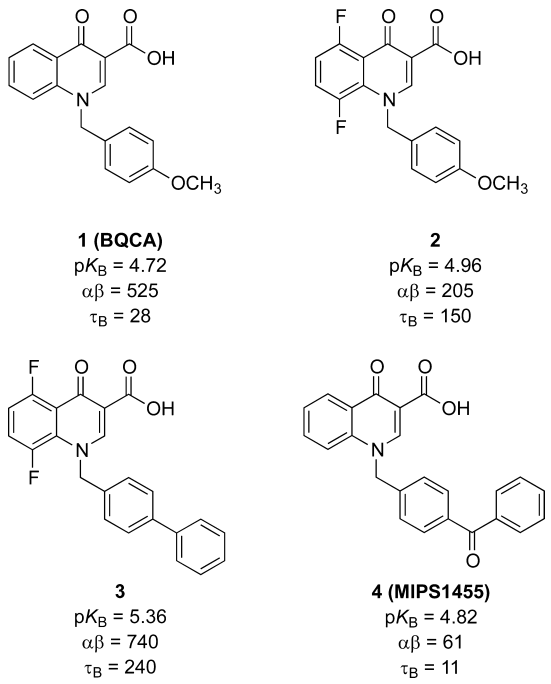

Figure 2. Structures of BQCA (**1**), two BQCA analogues (**2** and **3**), and the photoactivatable irreversible allosteric ligand MIPS1455 (**4**).

The extensive structure−activity relationship studies[16] performed on the parent molecule, the highly selective M_1 mAChR positive allosteric modulator benzyl quinolone carboxylic acid (BQCA, **1**, Figure 2),[17] guided our selection of the benzophenone group as our photoactivatable functionality. Many high potency BQCA analogues contain biaryl and fused aryl systems.[18−21] Specifically, replacement of the 4-methoxy group with a phenyl ring (**2** and **3**, Figure 2) resulted in improved affinity (pK_B), positive cooperativity ($\alpha\beta$), and allosteric agonism (τ_B).[22,23] This enabled us to confidently incorporate the benzophenone group into our ligand design without concern about steric disruption of the ligand−receptor binding interaction or functional activation.

Using [^{3}H]*N*-methylscopolamine (NMS) competition radioligand binding and ERK1/2 phosphorylaton assays performed at human M_1 mAChR-expressing Chinese hamster ovary (CHO) cells, we confirm that the allosteric binding and functional profile of BQCA, as well as the parent molecule's high mAChR subtype selectivity, is preserved in MIPS1455. Importantly, saturation radioligand binding assays using hM_1 mAChR-expressing CHO cell membranes reveal the ability of MIPS1455 to irreversibly bind to the receptor following photoactivation.

The quinolone carboxylic acid **5** was prepared in three steps as previously described.[24] Radical bromination of 4-methylbenzophenone gave a mixture of the desired monobrominated **6** and a small amount of dibrominated product. These compounds display a similar retention time and were unable to be separated by chromatographic methods. Fortunately, the crude mixture was successfully employed in the N-benzylation step to form the target molecule **4** in an acceptable yield (54%).

The allosteric binding and functional properties of BQCA (**1**) and MIPS1455 (**4**) were assessed, utilizing methods previously described,[24] by interacting the ligands with ACh in [^{3}H]NMS competition binding assays and ERK1/2 phosphorylation functional assays conducted in CHO cells stably expressing the hM_1 mAChR (Figure 3). MIPS1455 exhibited a similar affinity to BQCA (MIPS1455 K_B = 15 μM compared to BQCA K_B = 36 μM) and displayed positive binding (α = 61) and functional (β = 1.1) cooperativity with the agonist ACh and negative binding cooperativity with the antagonist [^{3}H]NMS (log $\alpha_{[NMS]}$ = −3.00) consistent with the two-state model of receptor activity reported for BQCA.[25] MIPS1455 also behaved as an allosteric agonist in its own right (MIPS1455 τ_B = 11 compared to BQCA τ_B = 28). [^{3}H]NMS competition binding curves and ERK1/2 phosphorylation concentration−response curves for BQCA and MIPS1455 in the absence of orthosteric agonist are available in Supporting Information Figure 1.

Next, we repeated the [^{3}H]NMS competition binding assays at the M_2-M_5 mAChR subtypes to evaluate the selectivity profiles of BQCA and MIPS1455. Neither significant positive cooperativity with ACh nor negative cooperativity with [^{3}H]NMS was observed with either ligand, suggesting that BQCA and MIPS1455 are unable to bind to, or else display neutral cooperativity with, the M_2-M_5 mAChRs (Supporting Information Figure 2).

Finally, we performed [^{3}H]NMS saturation membrane binding assays to ascertain whether MIPS1455 is capable of binding irreversibly to the M_1 mAChR. A protocol previously reported by our laboratory[24] was modified to incorporate a photoactivation step. Specifically, following a 1 h preincubation of M_1 mAChR-expressing CHO cell membranes with MIPS1455, the sample was exposed to 350 nm UV light for 30 min at 4 °C;[2] optimal conditions to affect photolysis, diradical formation, and covalent cross-linking by the benzophenone functionality (Figure 4).

[^{3}H]NMS saturation membrane binding assays revealed that MIPS1455 is binding irreversibly to the M_1 mAChR; a significant reduction in B_{max} (total receptor density) was observed following MIPS1455 preincubation and photoactivation compared to vehicle (B_{max} (% vehicle) = 50.2%; Figure 5A,D). This is indicative of reduced [^{3}H]NMS binding

dx.doi.org/10.1021/cn500173x | ACS Chem. Neurosci. 2014, 5, 902−907

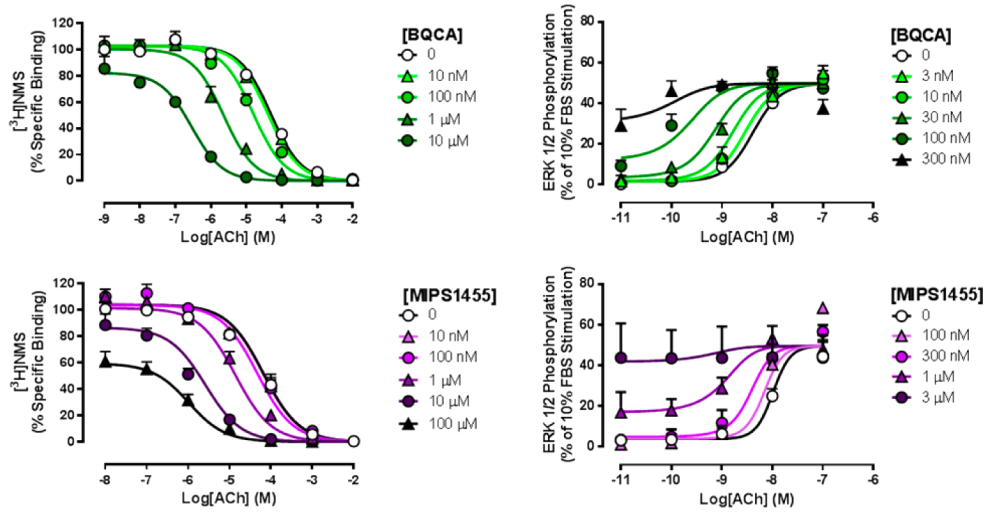

Figure 3. Pharmacological characterization of BQCA (**1**) and MIPS1455 (**4**) in a [^{3}H]NMS-ACh competition binding assay (left) and an ERK1/2 phosphorylation functional assay (right). Experiments performed in hM$_1$ mAChR-expressing CHO cells in the presence of increasing concentrations of ACh with or without increasing concentrations of BQCA (**1**) or MIPS1455 (**4**) (and, in the case of the binding assay, in the presence of a K_D concentration of radiolabeled orthosteric antagonist [^{3}H]NMS (0.1 nM)). The binding cooperativity factor between [^{3}H]NMS and each allosteric ligand was constrained to an arbitrary low value (log $\alpha_{[NMS]} = -3.00$) consistent with very high negative cooperativity. Values represent the mean ± SEM from at least three experiments performed in duplicate.

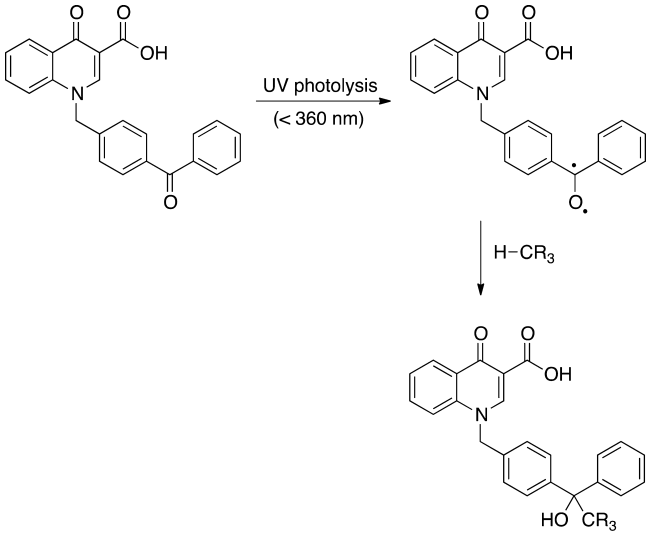

Figure 4. Scheme depicting UV photolysis, generation of a diradical intermediate, and covalent bond formation by a benzophenone functionality.

as a result of irreversible allosteric site occupation by MIPS1455, with which the radioligand has high negative cooperativity. No significant difference in B_{max} was observed following UV exposure of membranes preincubated with BQCA (B_{max} (% vehicle) = 88.6%, Figure 5B,D). Importantly, no change in B_{max} was observed following preincubation with MIPS1455 if the UV exposure step was omitted (B_{max} (% vehicle) = 90.3%, Figure 5C,D).

Herein we report the development of MIPS1455, a photoactivatable allosteric ligand for the M$_1$ mAChR. The synthesis of the ligand was completed following previously established methods (Scheme 1). In vitro [^{3}H]NMS competition binding assays and ERK1/2 phosphorylation functional assays confirmed that MIPS1455, like the parent molecule BQCA, acts as an M$_1$ mAChR positive allosteric modulator (Figure 3). Importantly, we demonstrate that MIPS1455 is capable of binding irreversibly to the M$_1$ mAChR following photoactivation with 350 nm UV light (Figure 5).

We postulate that this ligand may possess advantageous properties compared to our previously reported irreversible allosteric ligand MIPS1262 (see the Supporting Information Figure 3 for structure),[2] which contains an electrophilic isothiocyanate moiety.[24] MIPS1262 is limited to reacting with nucleophilic amino acid residues such as cysteine, serine and lysine. Such a requirement may result in the ligand adopting a distinct binding pose from that of BQCA in the allosteric binding site in order to orient itself around such residues (which may in turn lead to stabilization of a different receptor conformation), making it difficult to extrapolate any structural or functional findings to BQCA. Furthermore, the isothiocyanate moiety of MIPS1262 is inherently reactive, increasing the likelihood that the ligand binds nonselectively to multiple sites on the M$_1$ mAChR, in addition to the BQCA allosteric binding site. In a more complex in vitro setting, this reactivity is also likely to result in considerable off-target binding. In contrast, the benzophenone MIPS1455 affords the advantages of temporal control of reactivity, the ability to rapidly cross-link with any neighboring methylene unit (within 3.1 Å[4]) once activated, and more closely mimicking the structure of higher potency BQCA analogues than does MIPS1262. Furthermore, we demonstrate that the high mAChR subtype selectivity of BQCA is preserved with MIPS1455 (Supporting Information Figure 2). While these experiments were performed with the "ground state", nonphotoactivated MIPS1455, the results suggest that this ligand has little to no affinity for the other mAChRs and the likelihood of it cross-linking with these receptors following photoactivation is greatly reduced. Taken together, while MIPS1262 may serve as a useful ligand for investigating allosteric interactions in a recombinant in vitro setting, MIPS1455 may likely be a more favorable pharmacological tool for selectively probing structural and functional allosteric interactions at the M$_1$ mAChR in both a recombinant and native in vitro setting.

dx.doi.org/10.1021/cn500173x | ACS Chem. Neurosci. 2014, 5, 902−907

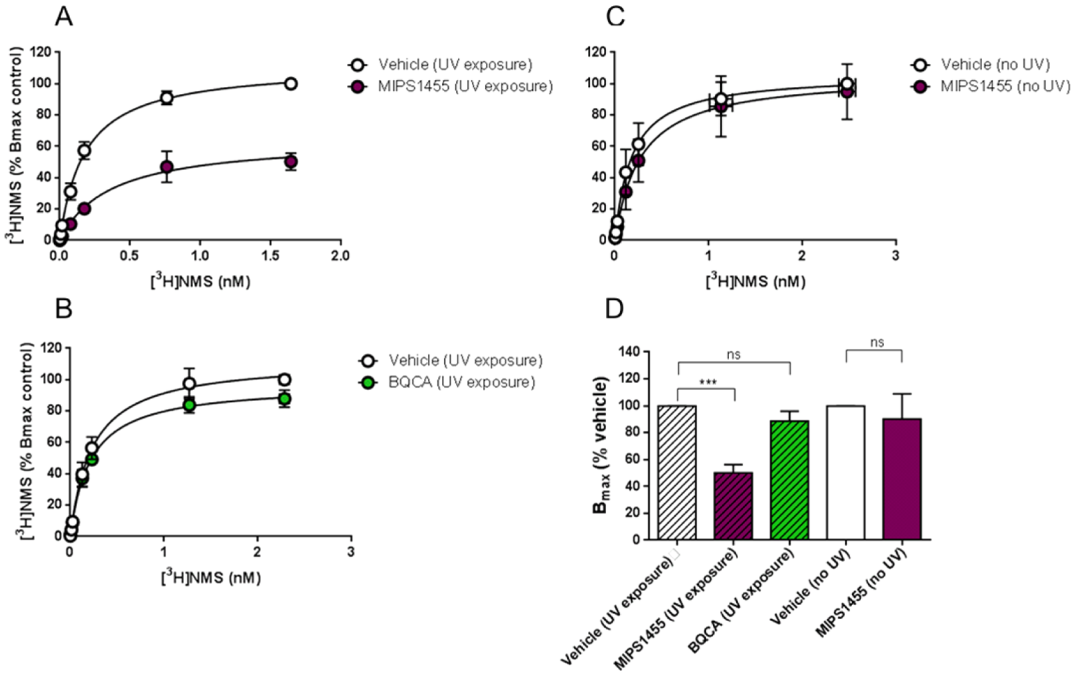

Figure 5. Pharmacological characterization of MIPS1455 (**4**) and BQCA (**1**) in [^{3}H]NMS saturation binding assays performed in hM$_1$ mAChR-expressing CHO cell membranes in the presence of increasing concentrations of radiolabeled orthosteric antagonist [^{3}H]NMS. (A) 1 h preincubation with vehicle or MIPS1455, followed by 30 min exposure to 350 nm UV light. (B) 1 h preincubation with vehicle or BQCA, followed by 30 min exposure to 350 nm UV light. (C) 1 h preincubation with vehicle or MIPS1455, without 30 min exposure to 350 nm UV light. (D) B_{max} (% vehicle) bar graphs where values significantly different from vehicle are indicated by asterisk(s) (*) (where * = $p < 0.05$, ** = $p < 0.01$, *** = $p < 0.001$, **** = $p < 0.0001$, and ns = not significant). Values represent the mean ± SEM from three experiments performed in duplicate.

Scheme 1. Synthesis of MIPS1455 (4)[a]

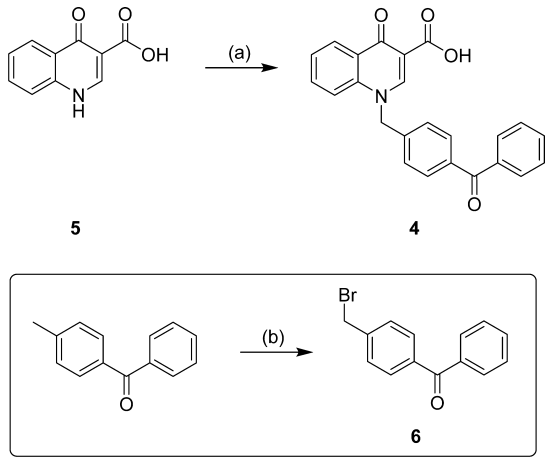

[a]Reagents and conditions: (a) **6**, DIPEA, ACN, 80 °C, 54%; (b) NBS, benzoyl peroxide, EtOAc, microwave 120 °C.

METHODS

Chemistry. *General.* All materials were reagent grade and purchased commercially from Sigma-Aldrich or Matrix Scientific. Anhydrous solvents were obtained from a MBraun MB SPS-800 Solvent Purification System. Analytical thin layer chromatography (TLC) was performed on silica gel 60 F_{254} precoated plates (0.25 mm, Merck ART 5554) and visualized by ultraviolet light, iodine, or ninhydrin as necessary. Silica gel 60 (Fluka) was used for silica gel flash chromatography. Microwave reactions were performed in a CEM Discover microwave reactor. Melting points (mp) were determined on a Mettler Toledo MP50 Melting Point System.

^{1}H NMR spectra were routinely recorded at 400 MHz using a Brüker Avancell Ultrashield Plus spectrometer equipped with a Silicon Graphics workstation. Chemical shifts (δ_H) for all ^{1}H NMR spectra are reported in parts per million (ppm) using the center peak of the deuterated solvent chemical shift as the reference: $CDCl_3$ (7.26) and d_6-DMSO (2.50).[26] Each resonance was assigned according to the following convention: chemical shift (δ) (multiplicity, coupling constant(s) in Hz, and number of protons). Coupling constants (J) are reported to the nearest 0.5 Hz. In reporting spectral data, the following abbreviations have been used: s, singlet; d, doublet; t, triplet; q, quartet; p, pentet; m, multiplet; br, broad; app, apparent; as well as combinations of these where appropriate.

^{13}C NMR spectra were routinely recorded at 100 MHz using a Brüker Avance 400 Ultra Shield Plus spectrometer equipped with a Silicon Graphics workstation. Chemical shifts (δ_C) for all ^{13}C NMR spectra are reported in parts per million (ppm), using the center peak of the deuterated solvent chemical shift as the reference: $CDCl_3$ (77.16) and d_6-DMSO (39.52).[26]

HSQC, HMBC, and COSY spectra were obtained using the standard Brüker pulse sequence to assist with structural assignment of the compounds.

Liquid chromatography–mass spectrometry (LCMS) was performed on an Agilent 1200 Series coupled to the 6120 quadrupole mass spectrometer. Elution was also monitored at 254 nm. High resolution mass spectrometry (HRMS) analyses were recorded in the specified ion mode using a LCT Premier XE TOF mass spectrometer coupled to a 2795 Alliance Separations Module at cone voltages of 45 V (ESI+) and 60 V (ESI−).

Analytical reverse-phase high performance liquid chromatography (HPLC) was performed on a Waters HPLC system using a Phenomenex Luna C8 (2) 100 Å column (150 × 4.6 mm, 5 μm) and a binary solvent system; solvent A, 0.1% TFA/H_2O; solvent B, 0.1% TFA/80% MeOH/H_2O. Isocratic elution was carried out using the following protocol (time, % solvent A, % solvent B): 0 min, 100, 0; 10 min, 20, 80; 11 min, 20, 80; 12 min, 100, 0; 20 min, 100, 0; at a flow rate of 1.0 mL/min monitored at 254 nm using a Waters 996 Photodiode Array detector.

dx.doi.org/10.1021/cn500173x | ACS Chem. Neurosci. 2014, 5, 902–907

Characterization requirements for intermediate compounds were set as mp, ^{1}H NMR, ^{13}C NMR, LCMS and HPLC (254 nm) or LCMS purity. Characterization requirements for final compounds were set as mp, ^{1}H NMR, ^{13}C NMR, LRMS, HRMS, and HPLC (254 and 214 nm) purity >95%.

*1-(4-Benzoylbenzyl)-4-oxo-1,4-dihydroquinoline-3-carboxylic Acid (**4**).* 4-Oxo-1,4-dihydroquinoline-3-carboxylic acid (180 mg, 952 μmol), crude 4-(bromomethyl)benzophenone (**6**) (393 mg, 1.43 mmol), and acetonitrile (8 mL) were placed in an RBF and cooled to 0 °C in an ice bath. *N*,*N*-Diisopropylethylamine (DIPEA) (4 equiv) was added, and the reaction stirred at 80 °C for 22 h. The reaction mixture was cooled to room temperature, and the precipitated product isolated as a white solid by vacuum filtration and washed with diethyl ether (197 mg, 54%); mp 235−236 °C. δ_H (d_6-DMSO) 15.15 (s, 1H), 9.36 (s, 1H), 8.43 (dd, J = 8.0, 1.0 Hz, 1H), 7.93−7.82 (m, 2H), 7.75−7.62 (m, 6H), 7.58−7.51 (m, 2H), 7.45 (d, J= 8.5 Hz, 2H), 6.02 (s, 2H). δ_C (d_6-DMSO) 195.1, 178.1, 165.9, 150.5, 140.2, 139.5, 136.8, 136.6, 134.3, 132.8, 130.2, 129.6, 128.6, 126.6, 126.5, 126.0, 125.7, 118.5, 108.1, 56.1. LCMS m/z [M + H]$^+$: 384.1. m/z HRMS (TOF ES$^+$) $C_{24}H_{17}NO_4$ [M + H]$^+$ calcd 384.1230, found 384.1226. HPLC: t_R = 9.88 min, purity (254) = 97.0%, purity (214) = 96.3%

*4-(Bromomethyl)benzophenone (**6**).* 4-Methylbenzophenone (200 mg, 1.02 mmol), *N*-bromosuccinimide (NBS) (218 mg, 1.22 mmol), and benzoyl peroxide (12.3 mg, 51 μmol) were placed in a microwave vial with ethyl acetate (4 mL), and the reaction mixture was stirred briefly to dissolve the reagents. The vessel was sealed and reacted in the microwave for 15 min at 120 °C. The reaction mixture was filtered to remove any precipitated NBS, and then the solvent evaporated in vacuo. The target molecule was reacted on without any further purification (crude mass: 577 mg); δ_H ($CDCl_3$) 7.76−7.69 (m, 4H), 7.46−7.39 (m, 5H), 4.47 (s, 2H). δ_C ($CDCl_3$) 178.4, 142.2, 137.4, 137.3, 132.7, 130.6, 130.4, 130.1, 129.0, 128.4, 126.6, 32.4. LCMS m/z [M(^{81}Br) + H]$^+$: 277.0. LCMS: t_R = 6.78 min, purity = 85.0% monobrominated product, 15.0% dibrominated byproduct.

Pharmacology. [^{3}H]NMS competition whole cell binding assays, ERK1/2 phosphorylation assays, and data analysis were performed as previously described.[24] [^{3}H]NMS saturation membrane binding assays were performed as follows.

Membrane Preparation. Prepreparred FlpIn-CHO cell membranes stably expressing human muscarinic M_1 receptors (hM_1 mAChR FlpIn-CHO) were thawed, diluted to a concentration of 1250 μg/mL, and resuspended using a hand-held homogenizer (at slow speed to minimize frothing). Ultracentrifuge tubes (one per buffer/ligand treatment) were labeled, 500 μg of membrane pipetted into each, the volume made up to 9 mL with cold HEPES-buffered saline, and the tubes kept on ice.

Preincubation with Controls and Test Ligands. Stock solutions of MIPS1455 and BQCA (10^{-2} M) were made up in DMSO. Ligands were diluted to 10^{-3} M in HEPES-buffered saline. A buffer control (10% DMSO/HEPES-buffered saline) was also made up. One milliliter buffer or ligand additions, for a final volume of 10 mL, were made, and the membrane tubes incubated in a water bath at 37 °C for 1 h. Membrane tubes were placed immediately on ice for 3 min and then exposed to 350 nm UV light at 4 °C for 30 min. Next, 10 mL of ice cold HEPES-buffered saline was added, and then additional ice cold buffer was added to bring all tubes to equal mass. Tubes were centrifuged on the Sorval ultracentrifuge at 4 °C for 20 min at 40 000 rpm. The supernatant was discarded, the membranes were washed and resuspended thoroughly in 1 mL of ice cold HEPES-buffered saline (to ensure the removal of any noncovalently bound ligand), an additional 19 mL of ice-cold buffer added, and the tubes brought to equal mass again. Tubes were centrifuged again on the Sorval ultracentrifuge at 4 °C for 20 min at 40 000 rpm. The supernatant was discarded, and the membranes resuspended in 400 μL of cold HEPES-buffered saline. A Bradford assay was performed to ascertain the concentration of membrane in each treatment tube, and then the required amount of cold HEPES-buffered saline was added to bring the concentration of each to 30 μg/mL.

Assay Protocol. Stock solutions of [^{3}H]NMS ($10^{-7.5}$ and 10^{-8} M) were made up in HEPES-buffered saline. Dilutions of [^{3}H]NMS were made up in HEPES-buffered saline at 10× the required concentration. A stock solution of atropine (10^{-4} M) was made up at 10× the required concentration. Membranes (100 μL per tube) were equilibrated at 37 °C for 1 h with 100 μL of HEPES-buffered saline (specific wells) or 100 μL of atropine (nonspecific wells) and 100 μL per well of each concentration of [^{3}H]NMS, in the required amount of HEPES-buffered saline to make a total volume of 1 mL per tube.

Assay Termination and Data Collection. Assays were terminated by harvesting the tubes in the Brandel harvester and rinsing tubes twice with 2 mL of ice-cold 0.9% NaCl solution. Membranes were dried under the heat lamp, picked, and placed into 6 mL scintillation tubes. Then 4 mL per tube of Ultima Gold scintillation liquid was added, and the tubes capped, vortexed, and left on the bench for 1 h at RT. The levels of bound radioligand, and therefore the degree of radioligand blockade by any irreversibly bound test ligands, was measured in disintegrations per minute (dpm) on the TriCarb 2910 TR liquid scintillation analyzer (PerkinElmer).

■ ASSOCIATED CONTENT

Supporting Information

(1) [^{3}H]NMS competition binding curves and ERK1/2 phosphorylation concentration−response curves for BQCA (**1**) and MIPS1455 (**4**) alone, (2) [^{3}H]NMS competition binding selectivity study of BQCA (**1**) and MIPS1455 (**4**) in hM_2−hM_5 mAChR-expressing CHO cells, "(3) structure of MIPS1262, and (4) HPLC chromatograms (254 and 214 nm) for compound **4**. This material is available free of charge via the Internet at http://pubs.acs.org.

■ AUTHOR INFORMATION

Corresponding Authors

*For P.J.S.: Phone: +61 (0)3 9903 9542. E-mail: Peter.Scammells@monash.edu.

*For A.C.: Phone: +61 (0)3 9903 9067. E-mail: Arthur.Christopoulos@monash.edu.

Author Contributions

The manuscript was written through contributions of all authors. All authors have given approval to the final version of the manuscript.

Author Contributions

B.J.D. conducted all of the experimentation, all authors contributed to experimental design and the production of the manuscript.

Funding

This research was supported by Discovery Grant DP110100687 of the Australian Research Council and Program Grant APP1055134 of the National Health and Medical Research Council (NHMRC) of Australia. A.C. and P.M.S. are Principal Research Fellows of the NHMRC.

Notes

The authors declare no competing financial interest.

■ ACKNOWLEDGMENTS

The authors would like to kindly thank Drs. Sebastian Furness and Karen Gregory for discussions that contributed to the experimental design.

■ ABBREVIATIONS

ACN, acetonitrile; BQCA, benzyl quinolone carboxylic acid (1-(4-methoxybenzyl)-4-oxo-1,4-dihydroquinoline-3-carboxylic acid); CHO, Chinese hamster ovary; COSY, correlation spectroscopy; DIPEA, *N*,*N*-diisopropylethylamine; DMSO, dimethyl sulfoxide; ERK, extracellular-regulated kinase; ESI,

electrospray ionization; GPCR, G protein-coupled receptor; HMBC, heteronuclear multiple-bond correlation; HPLC, high performance liquid chromatography; HRMS, high resolution mass spectrometry; HSQC, heteronuclear single quantum coherence; LCMS, liquid chromatography−mass spectrometry; LRMS, low resolution mass spectrometry; mAChR, muscarinic acetylcholine receptor; MP, melting point; NBS, *N*-bromosuccinimide; NMPB, *N*-methyl-4-piperidyl *p*-azidobenzilate; NMR, nuclear magnetic resonance; NMS, *N*-methylscopolamine; QNB, quinuclidinyl benzilate; RBF, round-bottomed flask; SEM, standard error of the mean; TFA, trifluoroacetic acid; TLC, thin layer chromatography; TOF, time-of-flight; UV, ultraviolet

REFERENCES

(1) Grunbeck, A., and Sakmar, T. P. (2013) Probing G Protein-Coupled Receptor−Ligand Interactions with Targeted Photoactivatable Cross-Linkers. *Biochemistry 52*, 8625−8632.

(2) Vodovozova, E. L. (2007) Photoaffinity Labeling and Its Application in Structural Biology. *Biochemistry 72*, 1−20.

(3) Gomes, I., Jordan, B. A., Gupta, A., Rios, C., Trapaidze, N., and Devi, L. A. (2001) G Protein Coupled Receptor Dimerization: Implications in Modulating Receptor Function. *J. Mol. Med. 79*, 226−242.

(4) Dorman, G., and Prestwich, G. D. (2000) Using photolabile ligands in drug discovery and development. *Trends Biotechnol. 18*, 64−77.

(5) Bin, X. U., and Ling, W. U. (2014) Analysis of Receptor-Ligand Binding by Photoaffinity Cross-Linking. *Sci. China Chem. 57*, 232−242.

(6) Lapinsky, D. J. (2012) Tandem Photoaffinity Labeling-Bioorthogonal Conjugation in Medicinal Chemistry. *Biorg. Med. Chem. 20*, 6237−6247.

(7) Brune, S., Pricl, S., and Wunsch, B. (2013) Structure of the σ_1 Receptor and Its Ligand Binding Site. *J. Med. Chem. 56*, 9809−9819.

(8) Benovic, J. L. (2012) G-Protein-Coupled Receptors Signal Victory. *Cell 151*, 1148−1150.

(9) Caulfield, M. P. (1993) Muscarinic Receptors- Characterization, Coupling and Function. *Pharmacol. Ther. 58*, 319−379.

(10) Langmead, C. J., Watson, J., and Reavill, C. (2008) Muscarinic Acetylcholine Receptors as CNS Drug Targets. *Pharmacol. Ther. 117*, 232−243.

(11) Moreno-Yanes, J. A., and Mahler, H. R. (1980) Photoaffinity Labeling of Specific Muscarinic Antagonist Binding Sites of Brain: I. Preliminary Studies Using Two p-Azidophenylacetate Esters of Tropine. *Biochem. Biophys. Res. Commun. 92*, 610−617.

(12) Amitai, G., Avissar, S., Balderman, D., and Sokolovsky, M. (1982) Affinity Labeling of Muscarinic Receptors in Rat Cerebral Cortex with a Photolabile Antagonist. *Proc. Natl. Acad. Sci. U.S.A. 79*, 243−247.

(13) Avissar, S., Amitai, G., and Sokolovsky, M. (1983) Oligomeric Structure of Muscarinic Receptors Is Shown by Photoaffinity Labeling: Subunit Assembly May Explain High- And Low-Affinity Agonist States. *Proc. Natl. Acad. Sci. U.S.A. 80*, 156−159.

(14) Gregory, K. J., Sexton, P. M., and Christopoulos, A. (2007) Allosteric Modulation of Muscarinic Acetylcholine Receptors. *Curr. Neuropharmacol. 5*, 157−167.

(15) Kruse, A. C., Kobilka, B. K., Gautam, D., Sexton, P. M., Christopoulos, A., and Wess, J. (2014) Muscarinic Acetylcholine Receptors: Novel Opportunities for Drug Development. *Nat. Rev. Drug Discovery 13*, 549−560.

(16) Davie, B. J., Christopoulos, A., and Scammells, P. J. (2013) Development of M_1 mAChR Allosteric and Bitopic Ligands: Prospective Therapeutics for the Treatment of Cognitive Deficits. *ACS Chem. Neurosci. 4*, 1026−1048.

(17) Ma, L., Seager, M. A., Wittman, M., Jacobson, M., Bickel, D., Burno, M., Jones, K., Graufelds, V. K., Xu, G., Pearson, M., McCampbell, A., Gaspar, R., Shughrue, P., Danziger, A., Regan, C., Flick, R., Pascarella, D., Garson, S., Doran, S., Kreatsoulas, C., Veng, L., Lindsley, C. W., Shipe, W., Kuduk, S., Sur, C., Kinney, G., Seabrook, G. R., and Ray, W. J. (2009) Selective Activation of the M_1 Muscarinic Acetylcholine Receptor Achieved by Allosteric Potentiation. *Proc. Natl. Acad. Sci. U.S.A. 106*, 15950−15955.

(18) Kuduk, S. D., Di Marco, C. N., Chang, R. K., Ray, W. J., Ma, L., Wittman, M., Seager, M. A., Koeplinger, K. A., Thompson, C. D., Hartman, G. D., and Bilodeau, M. T. (2010) Heterocyclic Fused Pyridone Carboxylic Acid M_1 Positive Allosteric Modulators. *Bioorg. Med. Chem. Lett. 20*, 2533−2537.

(19) Kuduk, S. D., DiPardo, R. M., Beshore, D. C., Ray, W. J., Ma, L., Wittman, M., Seager, M. A., Koeplinger, K. A., Thompson, C. D., Hartman, G. D., and Bilodeau, M. T. (2010) Hydroxy Cycloalkyl Fused Pyridone Carboxylic Acid M_1 Positive Allosteric Modulators. *Bioorg. Med. Chem. Lett. 20*, 2538−2541.

(20) Kuduk, S. D., Di Marco, C. N., Cofre, V., Pitts, D. R., Ray, W. J., Ma, L., Wittman, M., Veng, L., Seager, M. A., Koeplinger, K., Thompson, C. D., Hartman, G. D., and Bilodeau, M. T. (2010) N-Heterocyclic Derived M_1 Positive Allosteric Modulators. *Bioorg. Med. Chem. Lett. 20*, 1334−1337.

(21) Kuduk, S. D., Di Marco, C. N., Cofre, V., Ray, W. J., Ma, L., Wittman, M., Seager, M. A., Koeplinger, K. A., Thompson, C. D., Hartman, G. D., and Bilodeau, M. T. (2011) Fused Heterocyclic M_1 Positive Allosteric Modulators. *Bioorg. Med. Chem. Lett. 21*, 2769−2772.

(22) Yang, F. V., Shipe, W. D., Bunda, J. L., Nolt, M. B., Wisnoski, D. D., Zhao, Z., Barrow, J. C., Ray, W. J., Ma, L., Wittman, M., Seager, M. A., Koeplinger, K. A., Hartman, G. D., and Lindsley, C. W. (2010) Parallel Synthesis of *N*-Biaryl Quinolone Carboxylic Acids as Selective M_1 Positive Allosteric Modulators. *Bioorg. Med. Chem. Lett. 20*, 531−536.

(23) Mistry, S. N., Valant, C., Sexton, P. M., Capuano, B., Christopoulos, A., and Scammells, P. J. (2013) Synthesis and Pharmacological Profiling of Analogues of Benzyl Quinolone Carboxylic Acid (BQCA) as Allosteric Modulators of the M_1 Muscarinic Receptor. *J. Med. Chem. 56*, 5151−5172.

(24) Davie, B. J., Valant, C., White, J. M., Sexton, P. M., Capuano, B., Christopoulos, A., and Scammells, P. J. (2014) Synthesis and Pharmacological Evaluation of Analogues of Benzyl Quinolone Carboxylic Acid (BQCA) Designed to Bind Irreversibly to an Allosteric Site of the M_1 Muscarinic Acetylcholine Receptor. *J. Med. Chem. 57*, 5405−5418.

(25) Canals, M., Lane, J. R., Wen, A., Scammells, P. J., Sexton, P. M., and Christopoulos, A. (2012) A Monod-Wyman-Changeux Mechanism Can Explain G Protein-coupled Receptor (GPCR) Allosteric Modulation. *J. Biol. Chem. 287*, 650−659.

(26) Gottlieb, H. E., Kotlyar, V., and Nudelman, A. (1997) NMR Chemical Shifts of Common Laboratory Solvents as Trace Impurities. *J. Org. Chem. 62*, 7512−7515.